Distinguishing between nonlinear channel transport and contact effects in organic FETs

B. H. Hamadani[a] , J. L. LeBoeuf[a], R. J. Kline[b], I. McCulloch[d], M. Heeney[d], C. A. Richter[a], L. J. Richter[c], and D. J. Gundlach[a]

[a] National Institute of Standards and Technology (NIST), Semiconductor Electronics Division, 100 Bureau Drive, MS 8120, Gaithersburg, MD 20899 [b] NIST, Polymers Division, MS 8541, Gaithersburg, MD 20899 [c] NIST, Surface and Microanalysis Science Division, MS 8372, Gaithersburg, MD 20899 [d] Merck Chemicals, Chilworth Science Park, Southampton S016 7QD, United Kingdom

ABSTRACT

We investigate charge injection and transport in organic field-effect transistors fabricated by using poly(2,5-bis(3-tetradecylthiophene-2-yl)thieno[3,2-b]thiophene) (pBTTT-C14) or poly(3-hexylthiophene) (P3HT) as the active polymer layer. We show that in high mobility devices where the channel resistances are low compared to the contact resistances, the device performance can be dominated by the metal/organic semiconductor (OSC) contacts. However, in sets of devices where the channel resistance is dominant over the contacts (usually the lower mobility devices), we see pronounced field dependence in the saturation regime mobilities consistent with a Poole-Frenkel model of charge transport within the channel. The field-dependent mobility in short-channel devices produces nonlinear output current-voltage characteristics which can be modeled consistently in the Poole-Frenkel framework.

Keywords: organic field-effect transistor, contact resistance, channel resistance, Poole-Frenkel effect

1. INTRODUCTION

The integration of solution-processable organic field-effect transistors (OFETs) into electronic applications will be facilitated by a better understanding of the mechanism of charge injection and transport in these devices. In the past few years, significant progress has occurred towards achieving this goal. Charge transport in organic semiconducting materials occurs via hopping or tunneling between localized states.[1] In OFETs, theoretical modeling based on variable range hopping in the tail of an energy-dependent density of localized states has been shown to be a viable explanation for the mechanism of charge motion in these devices.[2,3] However, other intrinsic bulk effects have also been observed in organic semiconducting devices. Of particular interest is the dependence of the mobility on the longitudinal source-drain electric field, also referred to as the Poole-Frenkel-like (PF) effect.[4] The origin of this effect, which has been observed in a variety of conducting and semiconducting polymers,[5-7] has been a subject of active investigation, and several models have been proposed, mainly pertaining to the presence of energetic (energy-dependent density of states) and spatial disorder in the system.[7]

The observation of the PF effect in OFETs has been reported previously.[8,9] However, since the contact effects in OFETs often play an important role,[10,11] care must be taken to distinguish contact-limited charge injection from bulk-limited charge transport. Both effects can produce nonlinear *IV* characteristics with similar field and temperature dependences. In this paper, we discuss the fundamental differences between both contact-limited and channel-dominated behavior in two sets of organic polymer thin-film transistors and show that, independent of the material set, the PF effect is suppressed in devices that show high mobilities and high contact to channel resistance ratios whereas the effect is strongly observed in systems with low contact to channel resistances. We also show that, for devices that clearly exhibit the PF effect, we can understand and consistently model the nonlinear output characteristics in short channel devices in the low drain voltage regime.

2. DEVICE FABRICATION AND CHARACTERIZATION

Devices are fabricated in a bottom-contact configuration (see Fig. 1) on a degenerately doped n+ silicon wafer to be used as a gate. The gate oxide is 200 nm of thermally grown SiO_2. Source and drain electrodes are patterned using photolithography. The electrodes are deposited by E-beam evaporation of 40 nm of Au, followed by liftoff (pBTTT devices analyzed in the context of the PF effect are from an older cast and have 5 nm of Ti adhesion layer followed by 45 nm of thermally evaporated Au). The device width is fixed at $W = 800$ μm, with channel lengths ranging from $L = 5$ μm to $L = 80$ μm.

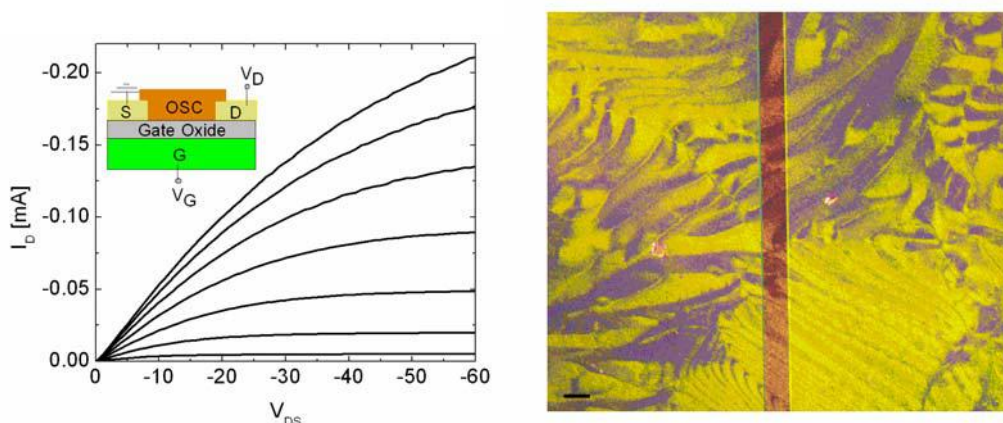

Figure 1. (left) The output characteristics of a pBTTT transistor with $L = 10$ μm and $W = 800$ μm. V_{GS} values from top to bottom are: -60 V to 0 V in steps of 10 V. (inset) Device cross section for a bottom-contact organic FET. (right) An optical image of the source/drain Au electrodes with the spin-cast pBTTT-C14 polymer on top, forming highly textured regions. AFM microscopy[15] of the films has revealed the formation of molecular-height terraced regions of 100 nm or more lateral size. Polarized microscopy of the films reveals that the microstructure seen above is highly birefringent, raising the possibility of the existence of coordinated grains that form domains tens of microns in length. The domains appear to cross the source-drain gap with no interruptions as seen above. The scale bar is 50 μm.

The polymer pBTTT-C14, was synthesized as previously reported[12] with number average relative molecular mass (M_n) and polydispersity of 28000 g/mol and 2.0, respectively. The pBTTT films were cast from a 3.5 mg/mL solution in chloroform:1,2 dichlorobenzene (8:1) at a rate of 3000 rpm onto substrates treated with octyltrichlorosilane (OTS). The gate dielectric was rendered hydrophobic by treatment with OTS. The as-cast (AC) pBTTT films upon annealing in a liquid-crystalline (LC) phase at elevated temperatures exhibit highly organized microstructure.[12] To achieve this phase, the AC devices were heated to 185 ºC on a hot plate for 5 min with a slow cool to room temperature. All processing occurred in a nitrogen or argon-purged glove box.

The polymer P3HT (as-received from Merck Chemicals)[13] was dissolved in chloroform at 1 mg/mL weight concentration and spun cast onto OTS treated substrates at a rate of 500 rpm. The Au electrodes for the P3HT devices were submerged in a 10 mM pentaflurobenzenethiol solution in ethanol for 30 min prior to OTS treatment in order to improve the contacts.[14] All processing and measurements were carried out in the argon glove box.

The devices operate as standard *p*-type FETs in accumulation mode. The device performance is evaluated by the effective linear (low drain voltage, V_{DS}) and saturation regime mobilities. In the low V_{DS} limit, the effective mobility is calculated from the relation:

$$I_D = \mu \frac{W}{L} C_i (V_{GS} - V_T) V_{DS},$$

(1)

and the effective saturation mobility, μ_{sat}, is extracted from:

$$I_{Dsat} = (1/2)\mu_{sat}(W/L)C_i(V_{GS} - V_T)^2,$$

(2)

by plotting and extracting the slope of $\sqrt{I_D}$ as a function of V_{GS} (the right-hand axis in Fig. 2). Here, C_i is the capacitance per unit area of the gate insulator (1.7×10^{-4} F/m^2), and V_T is the threshold voltage.

Figure 1 shows a plot of the output characteristics of a pBTTT transistor with L = 10 μm and W = 800 μm at several gate voltages, showing good saturation behavior at $V_{DS} > V_{GS} - V_T$. Figure 2 shows the transfer characteristics for an AC and LC pBTTT device, operating in saturation. The mobilities and the on-off ratios improve dramatically upon annealing the device in the LC phase. The high mobilities we have obtained in this system (≈ 0.63 cm^2/Vs) compare favorably to those reported in the literature (≈ 0.7 cm^2/Vs).[12]

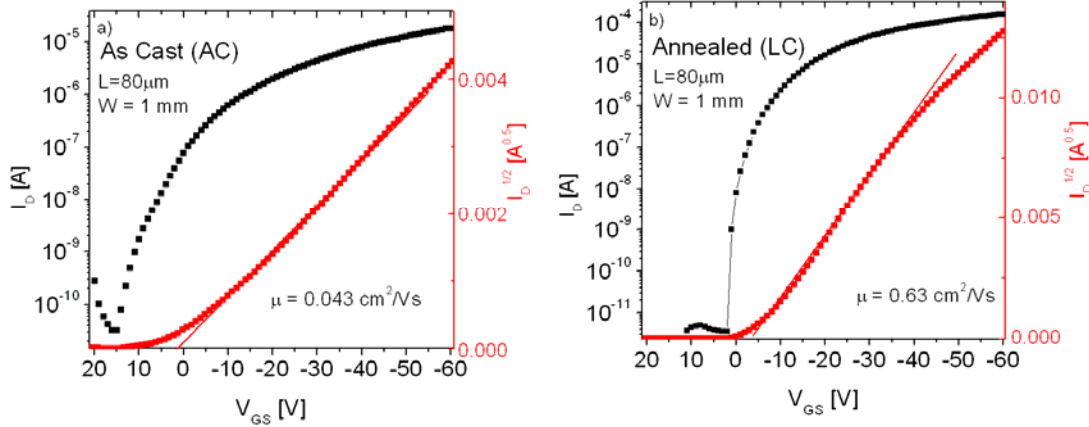

Figure 2. (a) The transfer characteristics of an as-cast pBTTT device at room temperature and V_{DS} = -60 V. (b) Same device after annealing in the LC phase, showing an improvement in mobility by an order of magnitude and on-off ratios greater than 10[7].

3. BULK VS CONTACT-LIMITED TRANSPORT

When examining the device characteristics of an OFET, one must consider whether the device performance is dominated by the channel resistance, R_{ch}, (related to intrinsic channel mobility) or by the combined parasitic resistance of the source/drain contacts, R_c. Although there are several well developed techniques to extract these two components, here we focus on the gated Transmission Line Model (TLM).[16] For a series of devices with fixed W, the total resistance, $R_{on} = \partial V_{DS} / \partial I_D$, is calculated at a small V_{DS} and plotted as a function of L for each gate voltage. Since $R_{on} = R_{ch}(L) + R_c$, the slopes of these plots at each V_{GS} gives R_{ch}/L, and the intercept extrapolated to $L = 0$ gives R_c.
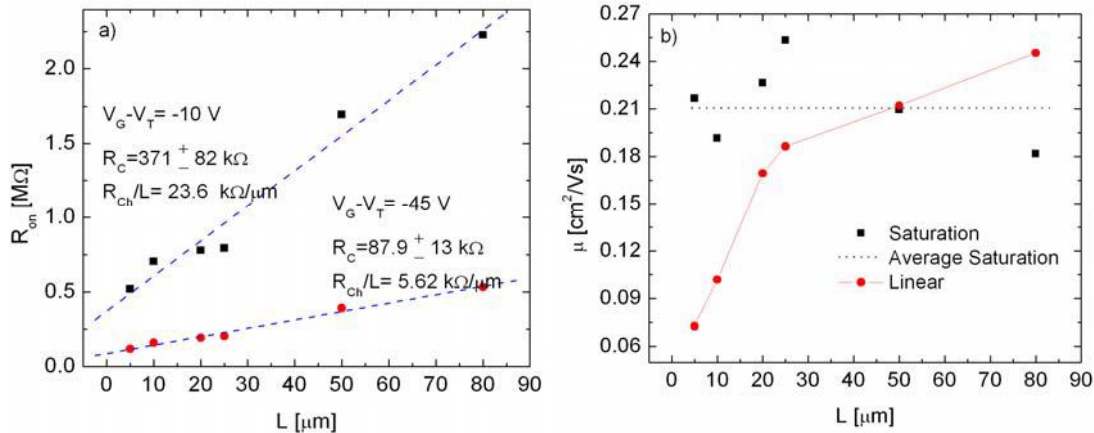

Figure 3. (a) Plot of R_{on} vs L for a series of pBTTT LC devices with W = 800 μm and two gate voltages corrected for the threshold voltage. (b) Plot of linear and saturation regime mobilities as a function of the channel length.
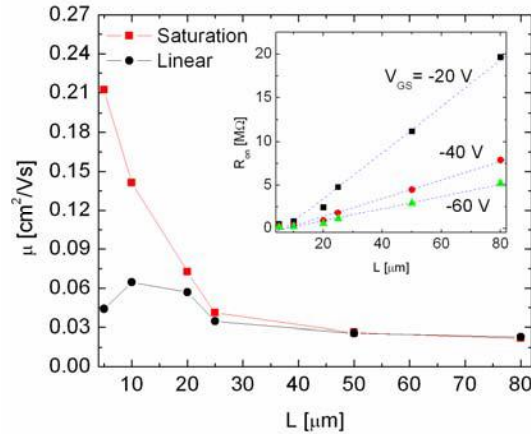
Figure 4. Plot of the saturation and linear regime mobilities as a function of L for a channel-limited pBTTT device. (inset) Plot of R_{on} vs L for this device at several gate voltages.

Figure 3a shows a plot of R_{on} vs L for a series of pBTTT LC devices with $W = 800$ μm and two gate voltages corrected for the threshold voltage. The extracted R_c and R_{ch}/L are shown on the graph and indicate that the device is contact-limited for channel lengths below ≈ 15 μm. Figure 3b shows a plot of linear and saturation mobilities as a function of channel length. The linear regime mobilities show a clear variation with L. This behavior of increasing effective mobility with increasing L has generally been observed in OFETs with contact issues,[10] consistent with the analysis of Fig. 3a.
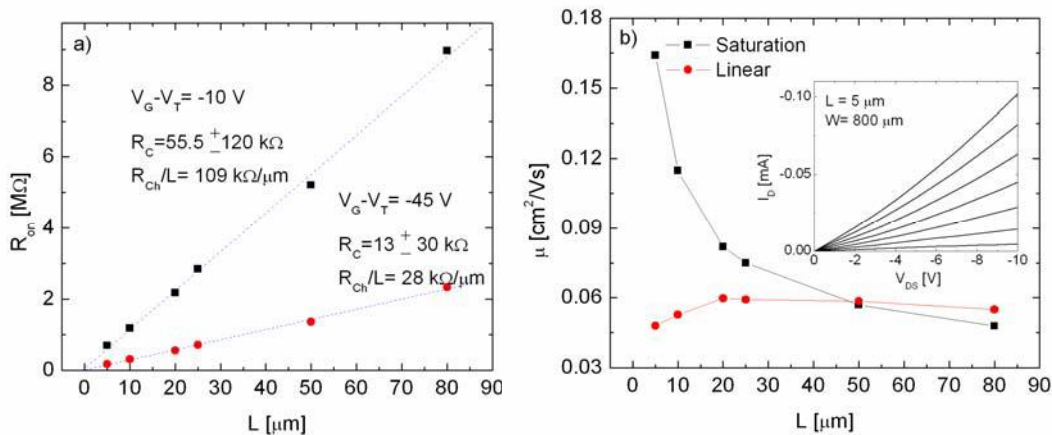

Figure 5. (a) Plot of R_{on} vs L for a series of P3HT devices with $W = 800$ μm and two gate voltages corrected for the threshold voltage. The analysis shows that, for the channel lengths investigated in this experiment ($L > 5$ μm), the contact resistances are much smaller than the channel resistances and therefore the charge transport and the device mobilities should be dominated by the bulk of the device. (b) Plot of the saturation and linear regime mobilities as a function of L. The linear regime mobilities are relatively independent of L, but the saturation mobility shows strong channel length dependence, decreasing with increasing channel length. (inset) Output characteristics of a short-channel P3HT device, showing nonlinear IV characteristics.

In contrast to the results of the analysis shown in Fig. 3, the data and a similar analysis for different pBTTT devices are presented in the main part of Fig. 4. Unlike the devices shown in Fig. 3, these pBTTT devices were fabricated with Au contacts evaporated onto Ti adhesion layers, and the processing entailed brief exposures to ambient air. The plot shows the saturation mobilities decreasing significantly as a function of L, with the linear regime mobilities relatively independent of L. The gated TLM analysis, shown in the inset for a few gate voltages, exhibits channel resistances in the range of 640 kΩ/μm to 70 kΩ/μm for the lowest and the highest gate voltages respectively, and no significant contact resistances. Similarly, Fig. 5a shows that the channel resistances are dominant over the contact resistances for even the shortest of our P3HT devices ($L = 5$ μm). From Fig 5b, we see that the linear regime mobilities are mostly constant across the spectrum of the channel lengths (similar to the channel-limited pBTTT devices), and the saturation mobilities

decrease by a factor of 4, from L = 5 µm to L = 80 µm. This trend is quite different from that observed in Fig. 3. We attribute the strong dependence of the saturation mobilities on L shown in Figs. 4 and 5 to the source-drain field dependence of the mobility or the so-called Poole-Frenkel like effect. The inset in Fig. 5b shows the output characteristics of a short channel P3HT device, showing nonlinear *IV* characteristics. In the PF model, the mobility is strongly proportional to the source-drain electric field and therefore nonlinear *IV* characteristics are expected, at least in the short channel devices. We will now investigate in more detail the effect of field-dependent mobility in our system.
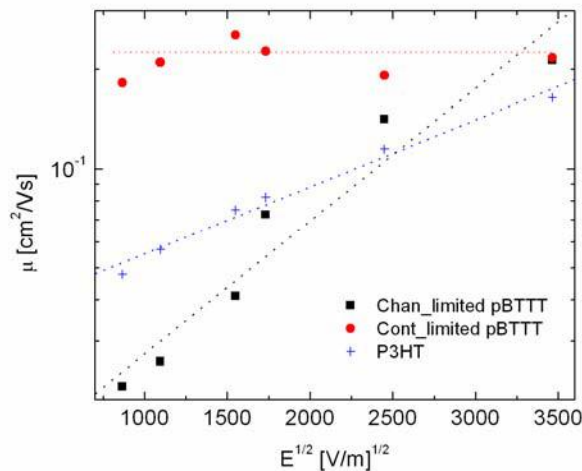

Figure 6. Log-linear plot of the saturation mobilities (V_{DS} = -60 V) vs $E^{1/2}$ for a set of channel-limited pBTTT, contact-limited pBTTT, and P3HT devices, with E defined as the average source-drain field given by V_{DS}/L. The channel-limited pBTTT shows the strongest dependence on the applied field.

4. ELECTRIC FIELD DEPENDENCE OF MOBILITY

In the set of devices where the contacts do not appear to play a dominant role (see Figs. 4 and 5), the channel length dependence of the saturation mobilities can be understood in terms of the more generally observed PF effect in organic semiconductors,[5-9] with the effective mobility given by:

$$\mu = \mu_0 \exp(\gamma \sqrt{E}),$$ (3)

where μ_0 is the zero-field mobility and the prefactor γ has been shown to depend inversely on T.[9] For our analysis, we assumed that E is given by V_{DS}/L, although this is not strictly true for a transistor operating in saturation. The justification for this assumption and a more complete analysis will be published elsewhere.[17]

Figure 6 shows a log-linear plot of the saturation mobilities vs $\sqrt{E}$ for a set of channel-limited pBTTT, contact-limited pBTTT, and the P3HT set of devices discussed earlier. These data fit reasonably well to the PF model. From the slope of the fits, the parameter γ can be extracted, with γ for the pBTTT devices being greater than the P3HT devices. (At room temperature, $\gamma_{(pBTTT\ LC)}$ = 0.0010 $(V/m)^{-1/2}$, and $\gamma_{(P3HT)}$ = 0.00046 $(V/m)^{-1/2}$). The contact-limited device shows no apparent trend with L. Notice that the channel-limited pBTTT devices at low fields have much lower mobilities than the contact-limited devices. This is because the channel resistances for these devices are much higher than the (more optimized) contact-limited devices. As T is lowered, the value of γ increases, proportional to $1/T$. This is due to the activated nature of transport in these systems. The increase in the value of γ with lower temperatures translates to stronger field dependence of the mobility, leading to an increase in nonlinearity of the low V_{DS} output characteristics with lower T.[17]

The origin of the PF effect is not well understood. Some recent experiments,[18,19] however, suggest that the presence of disorder at the grain boundaries may be responsible for the field dependence observed in the mobility. In order to invoke the PF effect in the transport characteristics, the field strength in the channel region should be high. The electric field in

the saturation regime (V_{DS} = -60 V) is much higher than in the linear regime; therefore the effect is more apparent for the saturation mobilities of the channel-limited devices across different L. In devices with lower R_{ch}, the performance becomes contact-limited, and there is little apparent PF effect in the extracted saturation mobilities. This is qualitatively consistent with the hypothesis that the PF effect originates from field-assisted hopping in a distribution of energetic disorder or defects at the grain boundaries. In the contact limited devices, the field in the channel is weak since a significant voltage is dropped across the contacts.[20] This may mask the PF effect, if a minimum field strength is needed to aid transport.

5. NONLINEAR *IV* MODELING

As it was mentioned earlier and shown in the inset of Fig. 4b, the short L (5 μm or 10 μm) channel-limited devices show nonlinearity in their low drain voltage output characteristics. If the mobility in our devices is given by Eq. 3, then we can model our device output characteristics by[21]:

$$I_D = \frac{\mu_0 W C_i}{L}\exp(\gamma\sqrt{V_{DS}/L})[(V_{GS}-V_T)V_{DS} - \frac{V_{DS}^2}{2}],\qquad(4)$$

where the mobility is replaced by Eq. 3. By using the γ values extracted from the saturation mobilities, as explained above, μ_0 is the only remaining fit parameter. The consistency of this model will depend on how good of a fit the extracted γ for each device set will produce pertaining to the (non)linearity of the I_D-V_{DS} plots and also how consistent the fit parameter μ_0 will be, if compared with low-drain mobility values extracted separately.
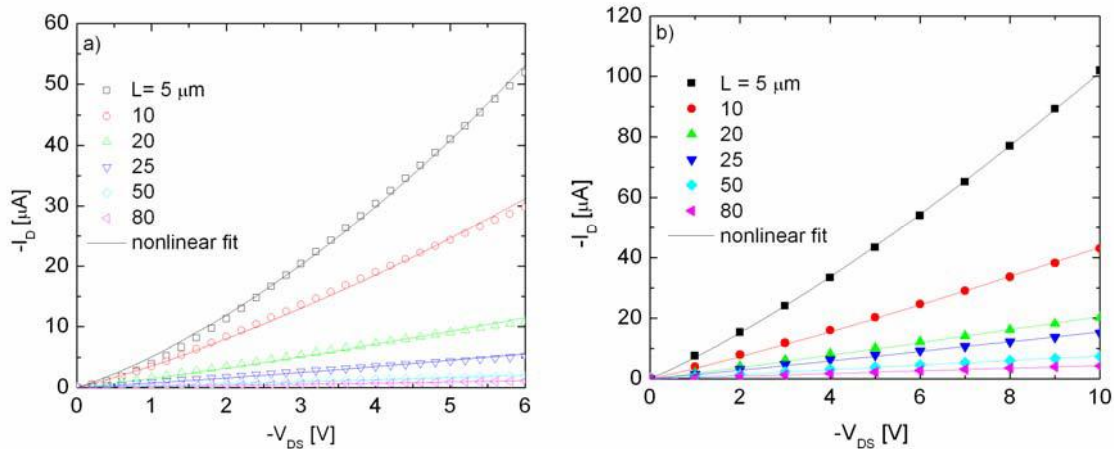

Figure 7. Plot of the transport characteristics of the channel-dominated pBTTT (a) and P3HT (b) device at low drain voltages and room temperature for several channel lengths and a fixed V_{GS} = -60 V. The two shortest channel lengths show nonlinearity in their output characteristics, whereas the rest of the devices show linear behavior. The lines are fits to the data, using the model of Eq. 4, closely reproducing the data.

Figure 7 shows the plot of the *IV* characteristics for the channel-limited pBTTT (a) and the P3HT transistors (b) at room temperature and fixed V_{GS} = -60 V for several channel lengths, with the nonlinear fits based on Eq. 4 shown by solid lines. The data fit well to the model with γ producing the nonlinear trend in the short channel devices and linear behavior for the longer ones. We find that the μ_0 values extracted from the fit, which physically should represent the device mobility in the zero-field limit, compare well with the effective linear regime mobilities. For example, the 5 μm device fit in the plot of Fig. 7a gives μ_0 = 0.021 cm^2/Vs, comparing favorably with an effective linear regime mobility of 0.025 cm^2/Vs. The same consistency is observed for the P3HT devices. These results indicate that this analysis is self-consistent, therefore providing a viable explanation for the field dependence and the nonlinear transport observed in these systems.

6. CONCLUSIONS

The issues related to charge injection and transport in OFETs has been recognized to be of great interest in the organic electronics community since understanding the outstanding problems of the subject will surely result in improvements in device fabrication and characterization techniques. In this work, we present our results of contact and channel resistance studies in two sets of polymeric devices, demonstrating that, depending on the influence of the contacts, different regimes of transport may be observed. In a contact-limited set of devices, the device mobilities either improved at higher channel lengths or showed no trend; however, the channel-dominated set of devices do show a strong channel length-dependent mobility. We relate this behavior to the Poole-Frenkel picture of a field-dependent mobility, and, based on this, we are able to model the nonlinear output characteristics observed in short channel devices. We believe that the presence of disorder at the grain boundaries is the cause of this field-dependent mobility behavior. Further studies with these systems, in particular at very short channel lengths, to find a direct correlation between the presence of grain boundaries and their influence on charge transport should lead to better understanding of charge carrier motion in these devices.

ACKNNOWLEDGEMENTS

REFERENCES

1. F. Gutmann and L. E. Lyons, *Organic Semiconductors,* John Wiley & Sons, Inc, 1967.
2. M. C. J. M. Vissenberg and M. Matters, "Theory of the field-effect mobility in amorphous organic transistors," *Phys. Rev. B* 57, 12964-12967 (1998).
3. E. J. Meijer, C. Tanase, P. W. M. Blom, E. van Veenendaal, B.-H. Huisman, D. M. de Leeuw, and T. M. Klapwijk, "Switch-on voltage in disordered organic field-effect transistors," *Appl. Phys. Lett.* 80, 3838-3840 (2002).
4. J. Frenkel, "On pre-breakdown phenomena in insulators and electronic semi-conductors," *Phys. Rev.* 54, 647-648 (1938).
5. W. D. Gill, "Drift mobilities in amorphous charge-transfer complexes of trinitrofluorenone and poly-n-vinylcarbazole," *J. Appl. Phys.* 43, 5033-5040 (1972).
6. P. W. M. Blom, M. J. M. de Jong, and M. G. van Munster, "Electric-field and temperature dependence of the hole mobility in poly(p-phenylene vinylene)," *Phys. Rev. B* 55, 656-659 (1997).
7. T. Kreouzis, D. Poplavskyy, S. M. Tuladhar, M. Campoy-Quiles, J. Nelson, A. J. Campbell, and D. D. C. Bradley, "Temperature and field dependence of hole mobility in poly(9,9-dioctylfluorene)," *Phys. Rev. B* 73, 235201 (2006).
8. P. Stallinga, H. L. Gomes, F. Biscarini, M. Murgia and D. M. de Leeuw, "Electronic transport in field-effect transistors of sexithiophene," *J. Appl. Phys.* 96, 5277-5283 (2004).
9. B. H. Hamadani and D. Natelson, "Gated nonlinear transport in organic polymer field effect transistors," *J. Appl. Phys.* 95, 1227-1232 (2004).
10. D. J. Gundlach, L. Zhou, J. A. Nichols, T. N. Jackson, P. V. Necliudov, and M. S. Shur, "An experimental study of contact effects in organic thin film transistors," *J. Appl. Phys.* 100, 024509 (2006).
11. B. H. Hamadani and D. Natelson, "Temperature-dependent contact resistances in high-quality polymer field-effect transistors," *Appl. Phys. Lett.* 84, 443-445 (2004).
12. I. McCulloch, M. Heeney, C. Bailey, K. Genevicius, I. MacDonald, M. Shkunov, D. Sparrowe, S. Tierney, R. Wagner, W. Zhang, M. L. Chabinyc, R. J. Kline, M. D. McGehee, and M. F. Toney, "Liquid-crystalline semiconducting polymers with high charge-carrier mobility," *Nat. Mat.* 5, 328-333 (2006).
13. NIST Disclaimer: Certain commercial equipment or materials are identified in this paper to foster understanding. Such identification does not imply recommendation or endorsement by the National Institute of Standards and Technology, nor does it imply that the materials or equipment identified are necessarily the best available for this purpose.

14. C-C Kuo, M. M. Payne, J. E. Anthony, and T. N. Jackson, "TES Anthradithiophene solution-processed OTFTs with 1 cm^2/V-s," *IEEE Inter. Elect. Dev. IEDM* 4, 373-376 (2004).

15. R. J. Kline, D. M. DeLongchamp, D. A. Fischer, E. K. Lin, M. Heeney, I. McCulloch, and M. F. Toney, "Significant dependence of morphology and charge carrier mobility on substrate surface chemistry in high performance polythiophene semiconductor films," *Appl. Phys. Lett.* 90, 062117 (2007).

16. S. M. Baier, M. S. Shur, K. Lee, N. C. Cirillo, Jr., and S. A. Hanka, "FET characterization using gated-TLM structure," *IEEE Tran. Elect. Dev.* ED-32, 2824-2829 (1985).

17. B. H. Hamadani, R. J. Kline, I. McCulloch, M. Heeney, C. A. Richter, and D. J. Gundlach, "Influence of source-drain electric field on mobility and charge transport in organic field-effect transistors," *J. Appl. Phys.* accepted (2007).

18. T. Minari, T. Nemoto, and S. Isoda, "Temperature and electric-field dependence of the mobility of a single-grain pentacene field-effect transistor," *J. Appl. Phys.* 99, 034506 (2006).

19. C. Goh, R. J. Kline, M. D. McGeheea, E. N. Kadnikova, and J. M. J. Fréchet, "Molecular-weight-dependent mobilities in regioregular poly(3-hexyl-thophene) diodes," *Appl. Phys. Lett.* 86, 122110-122112 (2005).

20. K. P. Puntambekar, P. V. Pesavento, and C. D. Frisbie, "Surface potential profiling and contact resistance measurements on operating pentacene thin-film transistors by Kelvin probe force microscopy," *Appl. Phys. Lett.* 83, 5539-5541 (2003).

21. A. C. Tickle, *Thin-Film Transistors*, John Wiley & Sons, Inc., New York, 1969.